Contribution from the Department of Chemistry,
Faculty of Science, Osaka City University, Osaka, 558 Japan

Binuclear Platinum(II) and -(III) Complexes of Pyridine-2-thiol and Its 4-Methyl Analogue. Synthesis, Structure, and Electrochemistry

Keisuke Umakoshi, Isamu Kinoshita, Akio Ichimura, and Shun'ichiro Ooi*

Received March 20, 1987

Reactions of *cis*-$PtCl_2(NH_3)_2$ with pyridine-2-thiol (pytH) in dioxane and $PtCl_2(CH_3CN)_2$ with potassium 4-methylpyridine-2-thiolate (4-mpytK) in toluene yield $[Pt_2(pyt)_4]$ (**1**) and $[Pt_2(4\text{-mpyt})_4]$ (**6**), respectively. Chloroform solutions of **1** and **6** give $[Pt_2Cl_2(pyt)_4]$ (**2**) and $[Pt_2Cl_2(4\text{-mpyt})_4]$ (**7**). The chloro ligand of **2** is substituted for other halide ions or thiocyanate to give $[Pt_2X_2(pyt)_4]$ (X = Br (**3**), I (**4**), SCN (**5**)) by the reaction of **2** with NaX. The structure of the binuclear Pt complex in the chloroform solvate of **2** and that in the toluene solvate of **6** have been investigated by X-ray diffraction. Two Pt atoms are bridged by four 4-mpyt ligands in $[Pt_2(4\text{-mpyt})_4]$, and two face-to-face planar *cis*-PtN_2S_2 units are related by a virtual twofold axis perpendicular to the Pt···Pt axis (Pt···Pt = 2.680 (2) Å). In $[Pt_2Cl_2(pyt)_4]$ the Cl atoms occupy the axial sites of the $Pt(pyt)_4Pt$ unit, which is structurally similar to $[Pt_2(4\text{-mpyt})_4]$. The Pt–Pt and Pt–Cl distances are 2.532 (1) and 2.458 (2) Å, respectively. Spectral and electrochemical features of **7** and **1** indicate that molecular structures of **7** and **1** resemble those of **2** and **6**. Compounds **1** and **6** show quasi-reversible cyclic voltammograms in DMF centered at +0.282 and +0.257 V vs. $Ag/Ag(Cryp(2,2))^+$, corresponding to $[Pt_2(L)_4] \rightleftharpoons [Pt_2(L)_4(dmf)_2]^{2+} + 2e^-$ (L = pyt, 4-mpyt). The cyclic voltammetry of $[Pt_2X_2(pyt)_4]$ is explained by the ECEC mechanism

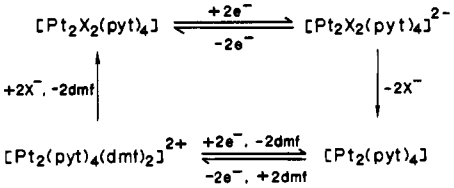

Crystal data: $[Pt_2(4\text{-mpyt})_4]\cdot C_7H_8$, monoclinic, space group $I2/a$, a = 22.001 (3) Å, b = 18.085 (2) Å, c = 16.532 (2) Å, β = 96.42 (1)°, Z = 8; $[Pt_2Cl_2(pyt)_4]\cdot 2CHCl_3$, monoclinic, space group $C2/c$, a = 22.167 (6) Å, b = 11.179 (2) Å, c = 14.917 (4) Å, β = 119.62 (2)°, Z = 4.

Introduction

Binuclear Pt^{III} complexes have attracted a considerable recent interest on account of the unusual oxidation state of platinum. They are classified into two groups: one has the $[XPt(B)_4PtX]^{n-}$ type structure (B = sulfate,[1] phosphates,[1c,2] pyrophosphite,[3] dithioacetates,[4] acetamide,[5] pyrimidine-2-thionate,[6] 2-thiouracilate;[6] X = neutral or univalent anion) and the other is of the $[XL_2Pt(B)_2PtL_2X]$ type (B = acetates,[7] α-pyridonate,[8] 1-methyluracilate;[9] X = neutral or univalent anion; L = ammonia or methyl group). Most of them were obtained either by reaction of the Pt^{II} complex with the bridging ligand at higher temperature under atmospheric oxygen or by oxidation of the precursor binuclear Pt^{II} complexes. Extensive studies on $[XPt(pop)_4PtX]^{4-}$ and $[X(NH_3)_2Pt(\alpha\text{-pyrd})_2Pt(NH_3)_2X]^{2+}$ have revealed the nature of tervalent platinum (pop = pyrophosphite; α-pyrd = α-pyridonate).

The Pt^{IV} and Pd^{II} complexes of 6-mercaptopurine are known to have antitumor activity.[10] We have attempted the synthesis of di- and tervalent Pt and Pd complexes of pyridine-2-thiol (pytH), which has the same kind of donor atoms as 6-mercaptopurine and a donor atom disposition similar to that of α-pyridone, anticipating that the stronger affinity of divalent platinum for sulfur than for oxygen makes the separation of possible isomers feasible. Although binuclear $[(en)Pt(pyt)_2Pt(en)]Cl_2$[11] and $[Pd(pyt)_4Pd]$[12] were obtained, an attempt to oxidize

(1) (a) Muraveiskaya, G. S.; Kukina, G. A; Orlova, V. S.; Evstaf'eva, O. N.; Porai-Koshits, M. A. *Dokl. Akad. Nauk SSSR* **1976**, *226*, 596–599. (b) Cotton, F. A.; Falvello, L. R.; Han, S. *Inorg. Chem.* **1982**, *21*, 2889–2891. (c) Bancroft, D. P.; Cotton, F. A.; Falvello, L. R.; Han, S.; Schwotzer, W. *Inorg. Chim. Acta* **1984**, *87*, 147–153.

(2) (a) Muraveiskaya, G. S.; Orlova, V. S.; Evstaf'eva, O. N. *Russ. J. Inorg. Chem. (Engl. Transl.)* **1974**, *19*, 561–565. (b) Muraveiskaya, G. S. Abashkin, V. E.; Evstaf'eva, O. N.; Golovaneva, I. F.; Shchelokov, R. N. *Sov. J. Coord. Chem. (Engl. Transl.)* **1981**, *6*, 218–225. (c) Cotton, F. A.; Falvello, L. R.; Han, S. *Inorg. Chem.* **1982**, *21*, 1709–1710. (d) Conder, H. L.; Cotton, F. A.; Falvello, L. R.; Han, S.; Walton, R. A. *Ibid.* **1983**, *22*, 1887–1891. (e) Cotton, F. A.; Han, S.; Conder, H. L.; Walton, R. A. *Inorg. Chim. Acta* **1983**, *72*, 191–193. (f) El-Mehdawi, R.; Bryan, S. A.; Roundhill, D. M. *J. Am. Chem. Soc.* **1985**, *107*, 6282–6286. (g) El-Mehdawi, R.; Fronczek, F. R.; Roundhill, D. M. *Inorg. Chem.* **1986**, *25*, 1155–1159. (h) El-Mehdawi, R.; Fronczek, F. R.; Roundhill, D. M. *Ibid.* **1986**, *25*, 3714–3716.

(3) (a) Che, C.-M.; Schaefer, W. P.; Gray, H. B.; Dickson, M. K.; Stein, P. B.; Roundhill, D. M. *J. Am. Chem. Soc.* **1982**, *104*, 4253–4255. (b) Che, C.-M.; Herbstein, F. H.; Schaefer, W. P.; Marsh, R. E.; Gray, H. B. *Ibid.* **1983**, *105*, 4604–4607. (c) Che, C.-M.; Mak, T. C. W.; Gray, H. B. *Inorg. Chem.* **1984**, *23*, 4386–4388. (d) Alexander, K. A.; Bryan, S. A.; Fronczek, F. R.; Fultz, W. C.; Rheingold, A. L.; Roundhill, D. M.; Stein, P.; Watkins, S. F. *Ibid.* **1985**, *24*, 2803–2808. (e) Hedden, D.; Roundhill, D. M.; Walkinshaw, M. D. *Ibid.* **1985**, *24*, 3146–3150. (f) Clark, R. J. H.; Kurmoo, M.; Dawes, H. M.; Hursthouse, M. B. *Ibid.* **1986**, *25*, 409–412. (g) Che, C.-M.; Lee, W.-M.; Mak, T. C. W.; Gray, H. B. *J. Am. Chem. Soc.* **1986**, *108*, 4446–4451. (h) Che, C.-M.; Mak, T. C. W.; Miskowski, V. M.; Gray, H. B. *Ibid.* **1986**, *108*, 7840–7841.

(4) (a) Bellitto, C.; Flamini, A.; Gastaldi, L.; Scaramuzza, L. *Inorg. Chem.* **1983**, *22*, 444–449. (b) Bellitto, C.; Bonamico, M.; Dessy, G.; Fares, V.; Flamini, A. *J. Chem. Soc., Dalton Trans.* **1986**, 595–601.

(5) Salyn, Ya. V.; Nefedov, V. I.; Mairova, A. G.; Kuznetsova, G. N. *Russ. J. Inorg. Chem. (Engl. Transl.)* **1978**, *23*, 458–460.

(6) (a) Goodgame, D. M. L.; Rollins, R. W.; Skapski, A. C. *Inorg. Chim. Acta* **1984**, *83*, L11–L12. (b) Goodgame, D. M. L.; Rollins, R. W.; Slawin, A. M. Z.; Williams, D. J.; Zard, P. W. *Inorg. Chim. Acta* **1986**, *120*, 91–101.

(7) Kuyper, J.; Vrieze, K. *Transition Met. Chem. (Weinheim, Ger.)* **1976**, *1*, 208–211. (b) Steele, B. R.; Vrieze, K. *Ibid.* **1977**, *2*, 169–174. (c) Schagen, J. D.; Overbeek, A. R.; Schenk, H. *Inorg. Chem.* **1978**, *17*, 1938–1940. (d) Bancroft, D. P.; Cotton, F. A.; Falvello, L. R.; Schwotzer, W. *Ibid.* **1986**, *25*, 763–770.

(8) (a) Hollis, L. S.; Lippard, S. J. *J. Am. Chem. Soc.* **1981**, *103*, 6761–6763. (b) Hollis, L. S.; Lippard, S. J. *Inorg. Chem.* **1982**, *21*, 2116–2117. (c) Hollis, L. S.; Lippard, S. J. *Ibid.* **1983**, *22*, 2605–2614. (d) Hollis, L. S.; Roberts, M. M.; Lippard, S. J. *Ibid.* **1983**, *22*, 3637–3644. (e) O'Halloran, T. V.; Roberts, M. M.; Lippard, S. J. *Ibid.* **1986**, *25*, 957–964.

(9) (a) Lippert, B.; Schöllhorn, H.; Thewalt, U. *Z. Naturforsch., B: Anorg. Chem., Org. Chem.* **1983**, *38B*, 1441–1445. (b) Lippert, B.; Schöllhorn, H.; Thewalt, U. *Inorg. Chem.* **1986**, *25*, 407–408. (c) Lippert, B.; Schöllhorn, H.; Thewalt, U. *J. Am. Chem. Soc.* **1986**, *108*, 525–526. (d) Schöllhorn, H.; Eisenmann, P.; Thewalt, U.; Lippert, B. *Inorg. Chem.* **1986**, *25*, 3384–3391.

(10) Kirschner, S.; Wei, Y.; Francis, D.; Bergman, J. G. *J. Med. Chem.* **1966**, *9*, 369.

(11) Kinoshita, I.; Yasuba, Y.; Matsumoto, K.; Ooi, S. *Inorg. Chim. Acta* **1983**, *80*, L13–L14.

(12) Umakoshi, K.; Kinoshita, I.; Ooi, S. *Inorg. Chim. Acta* **1987**, *127*, L41–L42.

0020-1669/87/1326-3551$01.50/0

them to tervalent metal complexes was unsuccessful. However, we recently found that $[Pt(pyt)_4Pt]$ obtained by the reaction of *cis*-$Pt(NH_3)_2Cl_2$ with pytH in organic solvent is readily oxidized to give $[ClPt^{III}(pyt)_4Pt^{III}Cl]$. This paper deals with the structures, chemical properties, and electrochemistry of the binuclear Pt^{II} and Pt^{III} complexes of pyridine-2-thiol and its analogue 4-methylpyridine-2-thiol (4-mpytH).

Experimental Section

Chemicals. Pyridine-2-thiol was purchased from Wako Pure Chemical Industries, Ltd., and 4-methylpyridine-2-thiol was prepared from 2-amino-4-picoline (Aldrich Chemical Co.) by the literature method.[13] They were recrystallized from benzene for use. *N,N*-Dimethylformamide (DMF) was dried over 3A molecular sieves and anhydrous copper sulfate and then distilled twice under reduced pressure. Tetrabutylammonium perchlorate (TBAP, Wako Pure Chemical Industries, Ltd.) was recrystallized twice from ethanol. Tetrabutylammonium bromide (Wako Pure Chemical Industries, Ltd.) was recrystallized twice from ethyl acetate. Benzyltriethylammonium chloride (Aldrich Chemical Co.) and tetrabutylammonium iodide (Wako Pure Chemical Industries, Ltd.) were used without further purification.

$[Pt_2(pyt)_4]$ (1). A suspension of *cis*-$[PtCl_2(NH_3)_2]$ (300 mg) in a dioxane solution of pyridine-2-thiol (222 mg/50 mL) was refluxed under argon atmosphere for 12 h with stirring. The color of the suspension gradually changed from yellow to lemon yellow during the refluxing. The crude product was collected, washed with dioxane and then water to remove ammonium chloride, and dried in vacuo; yield 320 mg (77%). The compound was recrystallized from hot DMF. Anal. Calcd for $C_{10}H_8N_2PtS_2$: C, 28.91; H, 1.79; N, 6.75. Found: C, 29.22; H, 1.72; N, 6.64.

$[Pt_2Cl_2(pyt)_4]$ (2). Compound **1** (300 mg) was dissolved in chloroform (300 mL) and stirred for 6 h at room temperature. Red parallelepiped crystals of $[Pt_2Cl_2(pyt)_4]\cdot 2CHCl_3$ (**2'**) were obtained by slow evaporation of the chloroform solution (yield 75%). The crystals of **2'** were pulverized gradually on standing by loss of chloroform. Compound **2** was obtained by removing chloroform in vacuo. Anal. Calcd for $C_{10}ClH_8N_2PtS_2$: C, 26.64; H, 1.79; N, 6.21. Found: C, 26.54; H, 1.72; N, 6.13.

$[Pt_2Br_2(pyt)_4]$ (3). (a) Synthesis from 2. A methanol solution of NaBr (1.0 g/15 mL) was added to the chloroform solution of **2** (41 mg/60 mL), and the mixture was stirred for 30 min. The red-orange solution was washed with water, dried over sodium sulfate, and evaporated slowly. Brown block crystals were washed with methanol and dried in vacuo; yield 44 mg (97%). Anal. Calcd for $BrC_{10}H_8N_2PtS_2$: C, 24.25; H, 1.63; N, 5.66. Found: C, 24.29; H, 1.62; N, 5.53.

(b) Synthesis from 1. A 50-mg amount of **1** was suspended in 50 mL of bromoform, and the mixture was stirred for 3 h at room temperature. A small amount of insoluble material was removed by filtration, and the red-orange filtrate was evaporated to dryness under reduced pressure. The red-brown residue was dissolved in 30 mL of chloroform. Brown platelike crystals were obtained by slow evaporation of solvent. They were washed with chloroform and dried in vacuo; yield 46 mg (77%). Anal. Calcd for $BrC_{10}H_8N_2PtS_2$: C, 24.25; H, 1.63; N, 5.66. Found: C, 23.85; H, 1.58; N, 5.29.

$[Pt_2I_2(pyt)_4]\cdot 2CHCl_3$ (4·2CHCl$_3$). A methanol solution of NaI (1.0 g/15 mL) was added to the chloroform solution of **2** (42 mg/60 mL), and the mixture was stirred for 30 min. The violet solution was washed with water, dried over sodium sulfate, and evaporated slowly. Dark violet crystals were washed with methanol and then a small amount of chloroform and dried in air; yield 55 mg (89%). Anal. Calcd for $C_{11}Cl_3H_9IN_2PtS_2$: C, 19.97; H, 1.37; N, 4.23. Found: C, 19.66; H, 1.29; N, 4.17.

$[Pt_2(SCN)_2(pyt)_4]$ (5). The ethanol solution of NaSCN (1.0 g/20 mL) was added to the chloroform solution of **2** (40 mg/60 mL), and the mixture was stirred for 2 h at room temperature. The red-orange solution was washed with water, dried over sodium sulfate, and evaporated slowly. Red block crystals were washed with ethanol and then a small amount of chloroform and dried in vacuo; yield 39 mg (92%). Anal. Calcd for $C_{11}H_8N_3PtS_3$: C, 27.90; H, 1.71; N, 8.88. Found: C, 27.97; H, 1.74; N, 8.75.

$[Pt_2(4\text{-mpyt})_4]\cdot C_7H_8$ (6·C$_7$H$_8$). A suspension of potassium 4-methylpyridine-2-thiolate (327 mg) in a toluene solution of $PtCl_2(CH_3CN)_2$ (307 mg/50 mL) was refluxed for 12 h under an argon atmosphere. The lemon yellow solid was filtered off from the red reaction mixture, which presumably contains some Pt^{III} species, washed with toluene and water, and dried in vacuo; yield 89 mg (20%). The product was recrystallized from hot toluene. Anal. Calcd for $C_{31}H_{32}N_4Pt_2S_4$: C, 38.03; H, 3.30; N, 5.72. Found: C, 38.27; H, 3.29; N, 5.65.

$[Pt_2Cl_2(4\text{-mpyt})_4]\cdot 0.5CHCl_3$ (7·0.5CHCl$_3$). This compound was obtained similarly to the synthesis of **2**; yield 75%. Anal. Calcd for $C_{24.5}Cl_{3.5}H_{24.5}N_4Pt_2S_4$: C, 28.92; H, 2.43; N, 5.51. Found: C, 29.20; H, 2.47; H, 5.34.

Table I. Crystallographic Data for X-ray Diffraction Studies

	$[Pt_2(4\text{-mpyt})_4]\cdot C_7H_8$	$[Pt_2Cl_2(pyt)_4]\cdot 2CHCl_3$
formula	$C_{31}H_{32}N_4Pt_2S_4$	$C_{22}Cl_8H_{18}N_4Pt_2S_4$
cryst syst	monoclinic	monoclinic
space group	$I2/a$	$C2/c$
a/Å	22.001 (3)	22.167 (6)
b/Å	18.085 (2)	11.179 (2)
c/Å	16.532 (2)	14.917 (4)
β/deg	96.42 (1)	119.62 (2)
V/Å^3	6537 (1)	3214 (1)
Z	8	4
d_{calcd}/(g cm^{-3})	1.81	2.36
cryst faces	100, $\bar{1}00$, 010, 0$\bar{1}$0, 01$\bar{1}$, 0$\bar{1}$1	01$\bar{1}$, 0$\bar{1}$1, 011, 0$\bar{1}\bar{1}$, 100, $\bar{1}$00
cryst size/mm	0.21 × 0.14 × 0.06	0.26 × 0.27 × 0.08
scan range/deg	1.0 + 0.4 tan θ	1.0 + 0.4 tan θ
scan mode	ω	ω–2θ
scan speed/(deg s^{-1})	0.033	0.025
bkgd estimation at each end of the scan/s	10	10
$2\theta_{max}$/deg	46.0	55.0
μ(Mo Kα)/cm^{-1}	92.8	100.8
transmission factor ranges	0.62–0.23	0.49–0.16
octants collected	$\pm h,+k,+l$	$\pm h,+k,+l$
unique rflns	4700	3880
obsd rflns with $I > 3\sigma(I)$	2348	2521
$R = \sum\|\|F_o\| - \|F_c\|\|/\sum\|F_o\|$	0.057	0.034
$R_w = [\sum w(\|F_o\| - \|F_c\|)^2/\sum w\|F_o\|^2]^{1/2}$	0.062	0.040

X-ray Structural Studies. Weissenberg photographs taken with Cu Kα radiation were used for investigating Laue symmetry, space group, and approximate unit-cell dimensions. Since the single crystal of **2'** is unstable in air as described above, it was sealed in a thin-walled glass capillary for use. The accurate cell dimensions were determined from the least-squares treatment of 16 (**2'**) and 20 (**6**) 2θ values of higher angle reflections ($14 \le 2\theta \le 26°$ (**2'**) and $14 \le 2\theta \le 24°$ (**6**)) measured on a Philips PW1100 diffractometer by use of Mo Kα radiation (λ = 0.71069 Å) at 295 ± 2 K (Table I). Intensities were measured on the diffractometer using graphite-monochromated Mo Kα radiation. For every crystal the intensities of three standard reflections ($\bar{4}02$, 040, 004 for **2'**; 10,0,0, 060, 006 for **6**) were monitored every 4 h, but they showed no appreciable decay during the data collection. The intensity data were corrected for absorption.[14]

The crystal structures were solved by the Patterson–Fourier method. The positional and thermal parameters were refined by the block-diagonal-matrix least-squares method. The minimized function was $\sum w(|F_o| - |F_c|)^2$, where $w = \sigma(F_o)^{-2}$. The refinement for the crystal structure of **2'** gave the R and R_w values shown in Table I. The structure refinement for **6** gave a very distorted toluene structure with large temperature factors, and therefore, in the subsequent refinement (full-matrix least squares),[15] the toluene molecule was treated as a rigid group on the assumption that C–C = 1.399 Å, C–CH$_3$ = 1.520 Å, and all atoms have the same isotropic temperature factor. Convergence was attained with the structure model in which each toluene molecule has a twofold disorder about the crystallographic twofold axis. In the final cycle of the refinement all parameter shifts were less than 0.1σ for both structures. No correction was made for secondary extinction. No attempt was made to locate hydrogen atoms in both structure analyses. Final difference syntheses showed no peak greater than 0.9 e Å^{-3} for **2'** and 1.5 e Å^{-3} for **6**.

The atomic scattering factors, with correction for anomalous dispersion of Pt^0, Cl^0, and S, were taken from ref 16. The computation was carried out by the FACOM 180II-AD computer at Osaka City Univ-

(13) (a) *Organic Syntheses*; Wiley: New York, 1965; Collect. Vol. 3, pp 136–138. (b) Thirtle, J. R. *J. Am. Chem. Soc.* **1946**, *68*, 342.

(14) Templeton, L. K.; Templeton, D. H. *Abstracts, American Crystallographic Association Proceedings*; American Crystallographic Association: Storrs, CT, 1973; Series 2, Vol. 1.

(15) Busing, W. R.; Martin, K. O.; Levy, H. A. "ORFLS"; Report ORNL-TM-305; Oak Ridge National Laboratory: Oak Ridge, TN, 1965.

(16) *International Tables for X-ray Crystallography*; Kynoch: Birmingham, England, 1974; Vol. IV.

Table II. Positional Parameters and Isotropic Temperature Factors[a]

A. $[Pt_2(4\text{-mpyt})_4]\cdot C_7H_8$

atom	x	y	z	B, Å²	atom	x	y	z	B, Å²
Pt(1)*	0.4349 (1)	0.4101 (1)	0.2653 (1)	4.48 (3)	C(33)	0.255 (1)	0.395 (1)	0.128 (2)	5.4 (6)
Pt(2)*	0.46033 (5)	0.4419 (1)	0.1144 (1)	4.18 (3)	C(34)	0.218 (1)	0.368 (2)	0.183 (2)	7.1 (8)
S(1)*	0.5347 (3)	0.4369 (5)	0.3104 (4)	6.5 (3)	C(35)	0.248 (1)	0.348 (2)	0.259 (2)	6.4 (7)
S(2)*	0.4593 (4)	0.2894 (4)	0.2450 (4)	6.1 (3)	C(36)	0.310 (1)	0.358 (2)	0.281 (2)	6.3 (7)
S(3)*	0.3571 (3)	0.4440 (4)	0.0742 (4)	5.9 (2)	C(37)	0.147 (1)	0.358 (2)	0.164 (2)	7.8 (8)
S(4)*	0.4607 (4)	0.5642 (4)	0.1466 (5)	6.1 (3)	N(41)	0.4116 (9)	0.520 (1)	0.284 (1)	5.0 (5)
N(11)	0.5541 (9)	0.440 (1)	0.150 (1)	4.6 (4)	C(42)	0.425 (1)	0.577 (1)	0.233 (2)	5.0 (6)
C(12)	0.578 (1)	0.435 (1)	0.230 (2)	5.4 (6)	C(43)	0.413 (1)	0.651 (1)	0.249 (2)	5.2 (6)
C(13)	0.642 (1)	0.435 (1)	0.250 (2)	5.4 (6)	C(44)	0.382 (1)	0.663 (2)	0.324 (2)	6.7 (7)
C(14)	0.681 (1)	0.433 (2)	0.191 (2)	7.4 (8)	C(45)	0.370 (1)	0.604 (2)	0.374 (2)	6.4 (7)
C(15)	0.654 (1)	0.438 (2)	0.109 (2)	6.7 (7)	C(46)	0.383 (1)	0.532 (2)	0.351 (2)	5.8 (7)
C(16)	0.590 (1)	0.438 (1)	0.088 (2)	5.4 (6)	C(47)	0.368 (1)	0.747 (2)	0.341 (2)	7.0 (7)
C(17)	0.751 (2)	0.426 (2)	0.216 (2)	8.4 (9)	TC(1)[b]	0.25	0.425 (2)	0.5	17. (1)
N(21)	0.4634 (8)	0.329 (1)	0.085 (1)	4.3 (4)	TC(2)	0.3021 (4)	0.386 (2)	0.533 (1)	17. (1)
C(22)	0.464 (1)	0.272 (1)	0.142 (1)	4.2 (6)	TC(3)	0.3021 (4)	0.309 (2)	0.533 (1)	17. (1)
C(23)	0.466 (1)	0.198 (1)	0.119 (2)	5.6 (6)	TC(4)	0.25	0.270 (2)	0.5	17. (1)
C(24)	0.474 (1)	0.182 (2)	0.038 (2)	5.9 (7)	TC(5)	0.3589 (8)	0.428 (2)	0.568 (3)	17. (1)
C(25)	0.475 (1)	0.241 (2)	−0.018 (2)	5.8 (7)	TC(6)	0.25	0.676 (2)	0.5	20. (1)
C(26)	0.470 (1)	0.313 (1)	0.004 (2)	5.4 (6)	TC(7)	0.2977 (6)	0.715 (2)	0.545 (1)	20. (1)
C(27)	0.481 (1)	0.102 (2)	0.012 (2)	7.7 (8)	TC(8)	0.2977 (6)	0.792 (2)	0.545 (1)	20. (1)
N(31)	0.3455 (9)	0.389 (1)	0.226 (1)	5.3 (5)	TC(9)	0.25	0.831 (2)	0.5	20. (1)
C(32)	0.317 (1)	0.405 (1)	0.151 (1)	4.5 (5)	TC(10)	0.350 (1)	0.673 (2)	0.593 (3)	20. (1)

B. $[Pt_2Cl_2(pyt)_4]\cdot 2CHCl_3$

atom	x	y	z	B(eq), Å²	atom	x	y	z	B(eq), Å²
Pt	0.05435 (2)	0.26356 (3)	0.33762 (2)	1.83 (1)	C(22)	−0.0737 (5)	0.4366 (7)	0.3028 (6)	2.7 (3)
Cl	0.1506 (1)	0.2750 (2)	0.5161 (2)	3.38 (7)	C(23)	−0.1109 (5)	0.5164 (8)	0.3318 (7)	2.8 (3)
N(11)	−0.0909 (4)	0.1081 (6)	0.1994 (5)	2.5 (3)	C(24)	−0.1820 (5)	0.5165 (9)	0.2764 (7)	3.5 (4)
C(12)	−0.0676 (5)	0.0733 (7)	0.2972 (7)	2.6 (3)	C(25)	−0.2167 (5)	0.4374 (8)	0.1937 (7)	3.2 (3)
C(13)	−0.0963 (5)	−0.0253 (8)	0.3209 (8)	3.2 (4)	C(26)	−0.1798 (4)	0.3650 (8)	0.1664 (7)	2.7 (3)
C(14)	−0.1477 (6)	−0.0903 (9)	0.2439 (8)	4.0 (4)	S(2)	0.0154 (1)	0.4359 (2)	0.3770 (2)	2.88 (8)
C(15)	−0.1718 (5)	−0.0543 (8)	0.1408 (8)	3.7 (4)	C	0.1095 (5)	0.2969 (9)	−0.0191 (8)	4.0 (4)
C(16)	−0.1419 (6)	0.0445 (8)	0.1228 (8)	3.8 (4)	Cl(1)	0.1669 (2)	0.2055 (3)	0.0832 (3)	6.3 (1)
S(1)	−0.0025 (1)	0.1515 (2)	0.4014 (2)	3.00 (8)	Cl(2)	0.1543 (2)	0.3606 (3)	−0.0770 (3)	6.3 (2)
N(21)	−0.1084 (4)	0.3655 (6)	0.2186 (5)	2.3 (2)	Cl(3)	0.0398 (2)	0.2129 (3)	−0.1106 (3)	6.7 (1)

[a] Atoms marked with an asterisk were refined anisotropically, and the equivalent isotropic temperature factors are listed in the table. [b] TC(1–5) and TC(6–10) denote the carbon atoms that constitute toluene groups A and B, respectively. An occupancy factor of 0.5 was assigned to TC(1), TC(4), TC(5), TC(6), TC(9), and TC(10). The esd's of positional parameters for TC atoms were calculated on the basis of the esd's of the orientation angles[15] ($\sigma(\rho)$ = 1.1° for A and 1.3° for B) and those of the coordinates of the origins for A and B (the origin was chosen as TC(4) for A and TC(9) for B).

ersity. Computational work was carried out by using ORFLS,[15] ORTEP,[17] and standard programs in UNICS.[18]

Electrochemical Measurements. Cyclic and rotating-disk-electrode (RDE) voltammetric measurements were performed with a Yanaco P-1100 system equipped with a Rika Denki RW-201K x-y recorder. RDE voltammetry was done with a Yanaco P10-RE rotator. The working and the counter electrodes were a glassy-carbon disk and a platinum wire, respectively. The $Ag/Ag(Cryp(2,2))^+$ (Cryp(2,2) = cryptand(2,2)) reference electrode[19] consisted of the half-cell having a salt bridge with fritted-glass junctions: Ag|0.005 M $AgClO_4$, 0.010 M Cryp(2,2), 0.05 M TBAP (DMF)||0.05 M TBAP (DMF)||. The reference electrode was checked periodically against the ferrocenium/ferrocene couple (Fc^+/Fc) in DMF. The Fc^+/Fc potential was +0.466 ± 0.001 V.

Controlled-potential coulometry was carried out in a standard H-type cell with a Hokuto HA-501 potentiostat and a Hokuto HF-201 coulometer. The working electrode was made of platinum gauze, and the working compartment was separated from the counter compartment by a sintered-glass disk.

Electrochemical measurements were performed at 25 ± 1 °C. The sample solutions (ca. 0.2 mM) containing 0.05 M TBAP as supporting electrolyte were deoxygenated with a stream of nitrogen. All potentials reported here are relative to the $Ag/Ag(Cryp(2,2))^+$ reference electrode.

Absorption Spectra. Spectra were recorded on a Hitachi 330 spectrophotometer at room temperature.

Results and Discussion

Synthesis and Characterization. The X-ray structure analysis disclosed that $6\cdot C_7H_8$ and **2′** are formulated as $[Pt^{II}_2(4\text{-mpyt})_4]\cdot C_7H_8$ and $[Pt^{III}_2Cl_2(pyt)_4]\cdot 2CHCl_3$, respectively. Compound **2**, obtained by removing chloroform from **2′**, therefore consists of $[Pt_2Cl_2(pyt)_4]$. An attempt to prepare single crystals of **1** was unsuccessful. Atomic coordinates are listed in Table II. Selected bond lengths and angles are given in Table III.

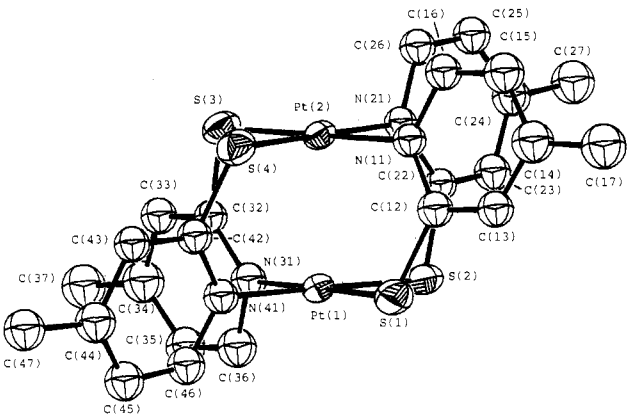

Figure 1. ORTEP diagram of $[Pt_2(4\text{-mpyt})_4]$ (30% probability contours for all atoms).

Both of the molecules have a twofold axis perpendicular to the Pt···Pt axis, though the twofold axis is an approximate one in **6** (Figures 1 and 2). The PtN_2S_2 coordination square has the cis configuration in both molecules. The two coordination squares in each molecule twist toward each other about the Pt···Pt axis; the N–Pt–Pt–S torsion angles in **6** and **2′** are in the 12.0 (6)–14.7 (6) and 22.6 (2)–24.0 (2)° ranges.

(17) Johnson, C. K. "ORTEP II", Report ORNL-5138; Oak Ridge National Laboratory: Oak Ridge, TN, 1976.
(18) "UNICS"; Crystallographic Society of Japan, Tokyo, 1969.
(19) Izutsu, K.; Ito, M.; Sarai, E. *Anal. Sci.* **1985**, *1*, 341–344.

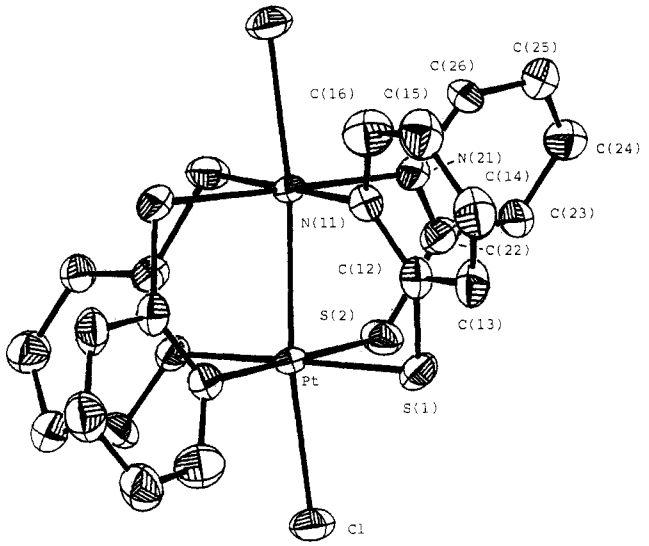

Figure 2. ORTEP diagram of $[Pt_2Cl_2(pyt)_4]$. Thermal ellipsoids are drawn at the 50% probability level.

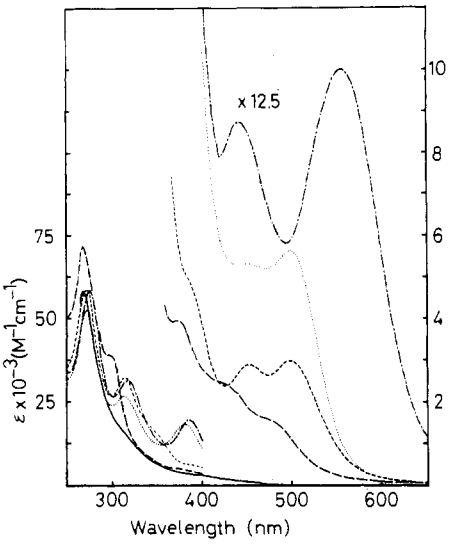

Figure 3. Absorption spectra of **1** in DMF (—) and **2** (– –), **3** (- - -), **4** (– · –), and **5** (···) in chloroform. Spectral data are as follows (λ_{max}, nm (ϵ_{max}, M^{-1} cm^{-1})): **1**, 267 (59 200), 312 (sh, 16 300); **2**, 267 (71 600), 298 (sh, 38 700), 375 (3980), 426 (sh, 2400), 473 (sh, 1500); **3**, 269 (59 300), 314 (32 900), 345 (sh, 17 000), 392 (sh, 4700), 452 (2830), 498 (2930); **4**, 274 (58 800), 317 (31 500), 384 (19 800), 444 (8900), 556 (10 000); **5**, 272 (52 700), 312 (26 900), 380 (18 400), 458 (5320), 498 (5640).

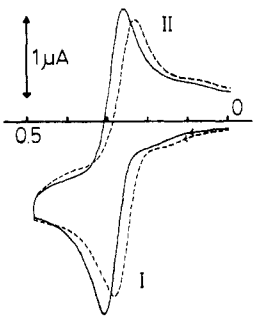

Figure 4. Cyclic voltammograms of 0.18 mM $[Pt_2(pyt)_4]$ (—) and 0.18 mM $[Pt_2(4\text{-mpyt})_4]$ (- - -) in 0.05 M TBAP–DMF at a glassy-carbon electrode with a scan rate of 20 mV s^{-1}.

The $Pt^{II}\cdots Pt^{II}$ distance in **6** (2.680 (2) Å) is the shortest among those so far reported. It is ca. 0.10 Å shorter than those in $[Pt_2(CH_3CSS)_4]$ (2.767 (1) Å)[20] and $[Pt_2((CH_3)_2CHCSS)_4]$ (2.795 (2) Å)[21] and 0.25 Å shorter than that in $K_4[Pt_2(pop)_4]\cdot 2H_2O$ (2.925 (1) Å).[22] The Pt^{III}–Pt^{III} bond length is comparable to those in $[Pt(pyd\text{-}2\text{-}t)_2Cl]_2$ (2.518 (1) Å),[6b] $(Et_4N)_2[Pt_2(H_2PO_4)_2(HPO_4)_2Cl_2]\cdot H_2O$ (2.529 (1) Å),[1c] and $[Pt_2(NH_3)_4(\alpha\text{-pyrd})_2Cl_2](NO_3)_2$ (2.5684 (5) Å)[8d] but 0.16 Å shorter than that in $K_4[Pt_2Cl_2(pop)_4]\cdot 2H_2O$ (2.695 (1) Å)[3b] (pyd-2-t = pyrimidine-2-thionate). As the N···S bite distance in the 4-mpyt ligand is not much different from that in the pyt ligand, the increase in the N–Pt–Pt–S torsion angle is responsible for the contraction of the Pt···Pt distance from $[Pt^{II}_2(4\text{-mpyt})_4]$ to $[Pt^{III}_2Cl_2(pyt)_4]$.

Both Pt–S and Pt–N bonds in $[Pt_2Cl_2(pyt)_4]$ are slightly longer than the corresponding ones in $[Pt_2(4\text{-mpyt})_4]$. Although the difference between Pt^{III}–L and Pt^{II}–L distances (L = S or N) is not significant from a statistical viewpoint, the Pt^{III}–P bonds in $K_4[Pt_2X_2(pop)_4]$ type complexes[3g] are also known to be >0.014 Å longer than the Pt^{II}–P bond in $K_4[Pt_2(pop)_4]\cdot 2H_2O$ (2.320 (5) Å).[22] The axial Pt^{III}–Cl bond is significantly longer than those in $K_4[Pt_2Cl_2(pop)_4]\cdot 2H_2O$ (2.407 (2) Å)[3b] but is comparable to those in $(Et_4N)_2[Pt_2(H_2PO_4)_2(HPO_4)_2Cl_2]\cdot H_2O$ (2.448 (1) Å)[1c] and $[Pt_2(NH_3)_4(\alpha\text{-pyrd})_2Cl_2](NO_3)_2$ (2.429 (4) Å).[8d]

The reaction of **6** with chloroform gives a red-brown compound with analytical formula $PtCl(4\text{-mpyt})_2\cdot 0.25CHCl_3$ (**7**). The electronic spectrum of **7** is very similar to that of **2**, indicating that **7** is composed of dinuclear $[Pt_2Cl_2(4\text{-mpyt})_4]$. Compound **7** reacts with sodium methoxide in DMF, and the recrystallization of the product from toluene gives a yellow crystalline compound (**6′**). Compound **6′** has the same analytical formula as **6** and shows a cyclic voltammogram identical with that of **6**. These facts indicate that **6** and **6′** are the same compounds. The chemical property of **1** having the analytical formula $Pt(pyt)_2$ is very similar to that of **6**; **1** affords **2** by the reaction with chloroform, and **2** reverts back to **1** by the reaction with sodium methoxide. The compound **1** exhibits a cyclic voltammogram similar to that of **6** (Figure 4), indicating that **1** is also composed of dimeric $[Pt_2(pyt)_4]$. In view of the longer Pt^{III}–Cl distance in **2** the Pt(bridge)$_4$Pt framework is held unchanged in the conversion reactions **1** ↔ **2** and **6** ↔ **7**. Thus, $[Pt_2(pyt)_4]$ and $[Pt_2Cl_2(4\text{-mpyt})_4]$ have structures similar to those of $[Pt_2(4\text{-mpyt})_4]$ and $[Pt_2Cl_2(pyt)_4]$, respectively.

As described above, $[Pt_2(pyt)_4]$ and $[Pt_2(4\text{-mpyt})_4]$ abstract chlorine atoms from solvent chloroform to give $[Pt_2Cl_2(pyt)_4]$ and $[Pt_2Cl_2(4\text{-mpyt})_4]$. These binuclear Pt^{II} complexes afford the bromo analogues of the corresponding Pt^{III} complexes by the reaction with bromoform but do not abstract halogen from other haloalkanes, e.g. dichloromethane, bromobenzene, and ethyl bromide.

Like the case of $[Pt_2Cl_2(pop)_4]^{4-}$,[23] the axial chloro ligands in $[Pt_2Cl_2(pyt)_4]$ are easily substituted for bromo, iodo, or thiocyanato ligands by reaction with an excess amount of alkali-metal halide or alkali-metal thiocyanate. $[Pt_2X_2(pyt)_4]$ (X = Br, I) may have a structure similar to that of $[Pt_2Cl_2(pyt)_4]$. The ν_{CN} bands (2115, 2128 cm^{-1}) for the NCS ligand in $[Pt_2(CNS)_2(pyt)_4]$ indicate that the NCS group is bonded to the Pt atom via a S atom.

Figure 3 shows the UV-visible spectra of $[Pt_2(pyt)_4]$ and $[Pt_2X_2(pyt)_4]$. The absorption at around 270 nm is common to the Pt^{II} and Pt^{III} complexes and hence attributable to the electronic transition localized on the pyt ligand. The intense absorption of the Pt^{III} complex in the 290–320-nm region is assignable to a $d\sigma \rightarrow d\sigma^*$ transition by analogy with the electronic transitions in $[Pt_2X_2(pop)_4]^{4-}$.[3a,g,24] The transition energy decreases in the order

(20) Bellitto, C.; Flamini, A.; Piovesana, O.; Zanazzi, P. F. *Inorg. Chem.* **1980**, *19*, 3632–3636.
(21) Bellitto, C.; Dessy, G.; Fares, V.; Flamini, A. *J. Chem. Soc., Chem. Commun.* **1981**, 409–411.
(22) Filomena Dos Remedios Pinto, M. A.; Sadler, P. J.; Neidle, S.; Sanderson, M. R.; Subbiah, A.; Kuroda, R. *J. Chem. Soc., Chem. Commun.* **1980**, 13–15.
(23) Bryan, S. A.; Dickson, M. K.; Roundhill, D. M. *J. Am. Chem. Soc.* **1984**, *106*, 1882–1883.
(24) Che, C.-M.; Butler, L. G.; Grunthaner, P. J.; Gray, H. B. *Inorg. Chem.* **1985**, *24*, 4662–4665.

Table III. Selected Bond Lengths, Bond Angles, and Torsion Angles for $[Pt_2(4\text{-mpyt})_4]\cdot C_7H_8$ ($\mathbf{6}\cdot C_7H_8$) and $[Pt_2Cl_2(pyt)_4]\cdot 2CHCl_3$ ($\mathbf{2'}$)[a]

	6	2'
Bond Lengths, Å		
Pt(1)–Pt(2)	2.680 (2)	2.532 (1)
Pt–Cl		2.458 (2)
Pt(2)–N(11)	2.08 (2)	2.103 (8)
Pt(2)–N(21)	2.11 (2)	2.106 (9)
Pt(1)–N(31)	2.04 (2)	
Pt(1)–N(41)	2.08 (2)	
Pt(1)–S(1)	2.289 (7)	2.291 (3)
Pt(1)–S(2)	2.281 (7)	2.304 (3)
Pt(2)–S(3)	2.293 (7)	
Pt(2)–S(4)	2.274 (7)	
C(12)–S(1)	1.72 (3)	1.744 (8)
C(22)–S(2)	1.74 (2)	1.722 (9)
C(32)–S(3)	1.77 (3)	
C(42)–S(4)	1.71 (3)	
N(11)···S(1)	2.74 (2)	2.705 (7)
N(21)···S(2)	2.75 (2)	2.706 (6)
N(31)···S(3)	2.73 (2)	
N(41)···S(4)	2.74 (2)	
Bond Angles, deg		
Pt(2)–Pt(1)–Cl		172.6 (1)
N(11)–Pt(2)–N(21)	89.4 (7)	88.5 (3)
N(11)–Pt(2)–S(4)	88.6 (5)	
N(21)–Pt(2)–S(3)	90.3 (5)	
S(3)–Pt(2)–S(4)	91.7 (3)	
N(31)–Pt(1)–N(41)	88.9 (7)	
N(31)–Pt(1)–S(2)	90.4 (6)	90.5 (2)
N(41)–Pt(1)–S(1)	89.6 (5)	91.1 (3)
S(1)–Pt(1)–S(2)	91.0 (3)	89.9 (1)
Pt(2)–N(11)–C(12)	122.1 (15)	122.2 (5)
Pt(2)–N(21)–C(22)	123.7 (14)	120.8 (7)
Pt(1)–N(31)–C(32)	125.8 (16)	
Pt(1)–N(41)–C(42)	123.0 (16)	
N(11)–C(12)–S(1)	124.0 (18)	121.9 (7)
N(21)–C(22)–S(2)	122.1 (16)	122.5 (8)
N(31)–C(32)–S(3)	121.5 (17)	
N(41)–C(42)–S(4)	124.0 (18)	
Pt(1)–S(1)–C(12)	109.9 (8)	106.7 (4)
Pt(1)–S(2)–C(22)	111.1 (8)	107.2 (3)
Pt(2)–S(3)–C(32)	110.0 (8)	
Pt(2)–S(4)–C(42)	109.4 (9)	
Torsion Angles, deg		
S(1)–Pt(1)–Pt(2)–N(11)	13.7 (6)	22.6 (2)
S(2)–Pt(1)–Pt(2)–N(21)	12.1 (5)	24.0 (2)
S(3)–Pt(2)–Pt(1)–N(31)	12.0 (6)	
S(4)–Pt(2)–Pt(1)–N(41)	14.7 (6)	

[a] The Pt(2), N(31), and N(41) atoms for **2'** stand for the atoms related to the Pt(1), N(21), and N(11) atoms, respectively, by the intramolecular twofold axis.

of X = Cl (298 nm) > SCN (312 nm) > Br (314 nm > I (317 nm), but the influence of the axial ligand on the transition energy is much less than that for $[Pt_2X_2(pop)_4]^{4-}$.

Electrochemistry. Figure 4 shows cylcic voltammograms of the compounds **1** and **6**. Both the compounds exhibit an electrochemically quasi-reversible oxidation process (peaks I and II) with $E_{1/2}$ = +0.282 V for **1** and +0.257 V for **6**. The anodic and cathodic peak separation (ΔE_p) varies with scan rate; e.g. ΔE_p = 37 mV at 5 mV s^{-1} and ΔE_p = 72 mV at 100 mV s^{-1}, indicating the quasi-reversible two-electron process. Controlled-potential coulometry for these complexes at +0.60 V gave an electron stoichiometry of 0.97 ± 0.05 e/Pt. The electrode reaction is therefore represented by

$$[Pt^{II}_2(L)_4] \rightleftharpoons [Pt^{III}_2(L)_4]^{2+} + 2e^- \qquad L = \text{pyt, 4-mpyt} \quad (1)$$

All Pt^{III} complexes characterized structurally have two axial ligands except for $[(NO_2)(NH_3)_2Pt(1\text{-MeU})_2Pt(NH_3)_2](NO_3)_3\cdot H_2O$ (1-MeU = 1-methyluracilate)[9c]: the Pt^{III} state seems to require some axial ligand for stabilization. The oxidation product $[Pt^{III}_2(L)_4]^{2+}$ may take up some ligands S from the outer coordination sphere to give $[Pt_2(L)_4(S)_2]^{2+}$. S may be either a solvent DMF molecule or perchlorate ion, but the former is more probable than the latter in view of the low coordination ability of the latter. So, the actual electrode reaction is expressed as

$$[Pt^{II}_2(L)_4] + 2S \underset{II}{\overset{I}{\rightleftharpoons}} [Pt^{III}_2(L)_4(S)_2]^{2+} + 2e^- \qquad S = \text{DMF} \quad (2)$$

The cyclic voltammograms of $[Pt^{III}_2X_2(pyt)_4]$ (X = Cl, Br, I, SCN) are shown in Figure 5. A negative-potential scan initiated at +0.5 V, where no Faradaic current is observed, gives the reduction peak III. The reverse positive scan from −0.7 V exhibits no appreciable reoxidation peak corresponding to the reduction peak III but gives a new oxidation peak at more positive potential. The peak potential of the reduction process shows a remarkable dependence on X and is −0.44 V for Cl, −0.32 V for Br, −0.24 V for SCN, and −0.23 V for I. On the other hand, the peak potential of the oxidation process has no dependence on X and is invariably +0.28 V, which is close to that of the oxidation peak for $[Pt_2(pyt)_4]$ (I in Figure 4). The RDE voltammetry of $[Pt_2X_2(pyt)_4]$ and $[Pt_2(pyt)_4]$ at 1000 rpm showed that the diffusion current for the reduction of the former is almost the same as that for the two-electron oxidation of the latter (reaction 2). These voltammetric results indicate the following electrochemical EC mechanism for the reduction of $[Pt_2X_2(pyt)_4]$:

$$[Pt^{III}_2X_2(pyt)_4] + 2e^- \rightleftharpoons [Pt^{II}_2X_2(pyt)_4]^{2-} \quad (3)$$

$$[Pt^{II}_2X_2(pyt)_4]^{2-} \rightarrow [Pt_2(pyt)_4] + 2X^- \quad (4)$$

Although the $[Pt_2(pyt)_4]$ thus formed is thought to be oxidized to give $[Pt_2(pyt)_4(S)_2]^{2+}$ according to reaction 2, the second cyclic scan does not give the expected rereduction peak II (the oxidation of $[Pt_2(pyt)_4]$) but gives only the reduction peak III. This implies that $[Pt_2(pyt)_4(S)_2]^{2+}$ reacts with X^-, which is liberated from $[Pt_2X_2(pyt)_4]$ upon the electrochemical reduction and still remains in the diffusion layer:

$$[Pt^{III}_2(pyt)_4(S)_2]^{2+} + 2X^- \rightarrow [Pt_2X_2(pyt)_4] + 2S \quad (5)$$

The following chemical reaction (5) is too fast to enable us to observe the definitive reduction peak even at −31 °C. However, a small but definitive reduction peak appeared at +0.20 V when 0.1 mL of methanol was added to the electrolytic solution (8 mL)

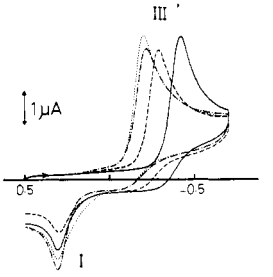

Figure 5. Cyclic voltammograms of 0.21 mM $[Pt_2X_2(pyt)_4]$ in 0.05 M TBAP–DMF at a glassy-carbon electrode with a scan rate of 50 mV s^{-1}, for X = Cl (—), Br (- - -), I (···), and SCN (–·–).

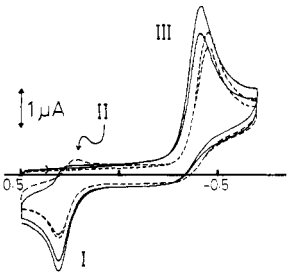

Figure 6. Cyclic voltammograms of 0.21 mM $[Pt_2Cl_2(pyt)_4]$ in the absence (—) and presence (- - -) of methanol in 0.05 M TBAP–DMF at a glassy-carbon electrode with a scan rate of 50 mV s^{-1} at 0 °C.

(25) Kondo, Y.; Shiotani, H.; Kusabayashi, S. *J. Chem. Soc., Faraday Trans. 1* **1984**, *80*, 2145–2153.

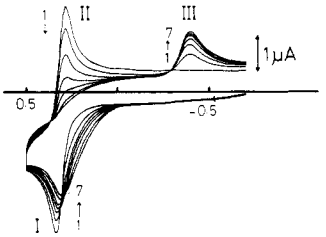

Figure 7. Effect of chloride ion on the cyclic voltammogram of $[Pt_2(pyt)_4]$ in 0.05 M TBAP-DMF at a glassy-carbon electrode with a scan rate of 50 mV s^{-1} and the following $[Cl^-]/[Pt_2]$ ratios: (1) 0; (2) 0.25; (3) 0.5; (4) 0.75; (5) 1.0; (6) 1.5; (7) 2.0.

Table IV. Peak Potentials (V) for the Oxidation and Reduction of $[Pt_2(pyt)_4]$ at Various Halide Ion Concentrations[a]

$[X^-]/[[Pt_2(pyt)_4]]$	E_p(I)	E_p(II)	E_p(III)
	X = Cl		
0	0.31	0.26	...
0.25	0.31	0.26	−0.43
0.5	0.30	0.26	−0.43
0.75	0.30	0.25	−0.43
1	0.29	...	−0.43
1.5	0.29	...	−0.43
2	0.28	...	−0.43
	X = Br		
2	0.28		−0.32
	X = I		
2	0.28		−0.23

[a] All measurements were performed at a scan rate of 50 mV/s.

(Figure 6). Undoubtedly this peak represents the reduction process in the redox couple $[Pt_2(pyt)_4]^{2+/0}$. Kondo and co-workers reported that the solvation of methanol to chloride ion diminishes the reaction rate of ethyl iodide with chloride ion in acetonitrile.[25] Methanol thus gives rise to a retardation of the substitution rate of reaction 5, resulting in the appearance of the cathodic peak.

Chloride ion gave a remarkable influence on the cyclic voltammograms of $[Pt_2(pyt)_4]$ (Figure 7). The increase in chloride ion concentration (as benzyltriethylammonium chloride) diminishes the reduction peak II and gives a new irreversible peak, the potential of which is equal to that of the reduction peak of $[Pt_2Cl_2(pyt)_4]$ (−0.43 V). Similar cyclic voltammograms were also obtained in the case of other halide ions. The peak potential of the new reduction peak coincides with that of the reduction peak for $[Pt_2X_2(pyt)_4]$. These observations indicate the fast substitution reaction of $[Pt_2(pyt)_4(S)_2]^{2+}$ with X^- to form $[Pt_2X_2(pyt)_4]$ in the diffusion layer. The peak potential for the oxidation of $[Pt_2(pyt)_4]$ shifts slightly from +0.31 V to the negative potential with increase of chloride ion concentration and reaches +0.28 V when the molar ratio of chloride ion to $[Pt_2(pyt)_4]$ becomes 2 (Table IV). The fact that this peak potential is exactly equal to that of $[Pt_2Cl_2(pyt)_4]$ gives evidence of formation of $[Pt_2(pyt)_4]$ upon the electrochemical reduction of $[Pt_2X_2(pyt)_4]$. The slight decrease in the oxidation peak current accompanied by the peak broadening with increase of chloride ion concentration may be attributed to the chemical reaction followed by the electrode process and the slight decrease in the heterogeneous electron-transfer rate. Similar cyclic voltammetric behavior was observed in the oxidation process of the binuclear complex $[Rh_2(dimen)_4]^{2+}$ (dimen = 1,8-diisocyanomethane) in the presence of chloride ion in aprotic solvent.[26] Although the peak potential for oxidation of $[Pt_2(pyt)_4]$ is independent of the coexistent halide ion, that for the oxidation of $[Pt_2(pop)_4]^{4-}$ shows a remarkable dependence on the halide ion.[27] Roundhill and co-workers attributed the halide ion dependence to the participation of the halide adduct of $[Pt_2(pop)_4]^{4-}$, $Pt_2(pop)_4X^{5-}$, to the electrode process.

The electrochemistry of $[Pt_2X_2(pyt)_4]$ thus far described can be summarized in the form of a four-component scheme or an ECEC mechanism:[28,29]

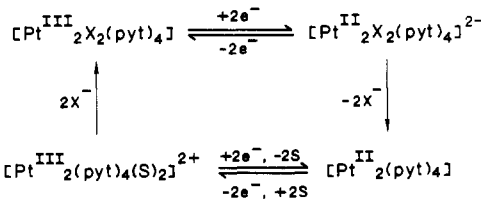

Acknowledgment. This work was supported by a Grant-in-Aid for Scientific Research (No. 58470037) from the Japanese Ministry of Education, Science and Culture. We are grateful to the reviewers of the paper for valuable suggestions on crystallography.

Registry No. **1**, 110173-35-8; **2**, 110173-36-9; 2^{2-}, 110173-43-8; **2′**, 110222-25-8; **3**, 110173-37-0; 3^{2-}, 110173-44-9; **4**, 110173-38-1; 4^{2-}, 110173-46-1; **5**, 110173-39-2; 5^{2-}, 110173-45-0; **6**·C_7H_8, 110173-41-6; **7**, 110173-47-2; *cis*-$[PtCl_2(NH_3)_2]$, 15663-27-1; $PtCl_2(CH_3CN)_2$, 13869-38-0; $[Pt_2(pyt)_4(DMF)_2]^{2+}$, 110173-42-7; $[Pt_2(4mpyt)_4(DMF)_2]^{2+}$, 110191-18-9; $CHCl_3$, 67-66-3; Pt, 7440-06-4; bromoform, 75-25-2.

Supplementary Material Available: Listings of thermal parameters (Tables SIA and SIB) and full lists of bond lengths and bond angles (Tables SIIA and SIIB) (9 pages); tables of calculated and observed structure factors (6 pages). Ordering information is given on any current masthead page.

(26) Rhodes, M. R.; Mann, K. R. *Inorg. Chem.* **1984**, *23*, 2053–2058.
(27) Bryan, S. A.; Schmehl, R. H.; Roundhill, D. M. *J. Am. Chem. Soc.* **1986**, *108*, 5408–5412.
(28) Geiger, W. E. *Prog. Inorg. Chem.* **1985**, *33*, 275–352.
(29) Bond, A. M.; Oldham, K. B. *J. Phys. Chem.* **1983**, *87*, 2492–2502.